

Journal of Materials Chemistry B

Accepted Manuscript



This article can be cited before page numbers have been issued, to do this please use: N. Depalo, V. De Leo, M. Corricelli, R. Gristina, G. Valente, E. Casamassima, R. Comparelli, V. Laquintana, N. Denora, E. Fanizza, M. Striccoli, A. Agostiano, L. Catucci and M. L. Curri, *J. Mater. Chem. B*, 2017, DOI: 10.1039/C6TB02590K.



This is an Accepted Manuscript, which has been through the Royal Society of Chemistry peer review process and has been accepted for publication.

Accepted Manuscripts are published online shortly after acceptance, before technical editing, formatting and proof reading. Using this free service, authors can make their results available to the community, in citable form, before we publish the edited article. We will replace this Accepted Manuscript with the edited and formatted Advance Article as soon as it is available.

You can find more information about Accepted Manuscripts in the [author guidelines](#).

Please note that technical editing may introduce minor changes to the text and/or graphics, which may alter content. The journal's standard [Terms & Conditions](#) and the ethical guidelines, outlined in our [author and reviewer resource centre](#), still apply. In no event shall the Royal Society of Chemistry be held responsible for any errors or omissions in this Accepted Manuscript or any consequences arising from the use of any information it contains.

Lipid Based Systems Loaded with PbS Nanocrystals Near Infrared Emitting Trackable Nanovectors

N. Depalo^{a†*}, V. De Leo^{a,b†*}, M. Corricelli^a, R. Gristina^c, G. Valente^{a,b}, E. Casamassima^b, R. Comparelli^a, V. Laquintana^d, N. Denora^d, E. Fanizza^b, M. Striccoli^a, A. Agostiano^{a,b}, L. Catucci^b, M. L. Curri^a

Received 00th January 20xx,
Accepted 00th January 20xx

DOI: 10.1039/x0xx00000x

www.rsc.org/

Hydrophobic PbS nanocrystals (NCs) emitting in the near infrared spectral region were encapsulated in the core of micelles and in the bilayer of liposomes, respectively, both formed of polyethylene glycol (PEG) grafted phospholipids. The phospholipid based functionalization process of PbS NCs required the replacement of the pristine capping ligand at the NC surface with thiol molecules. The procedures carried out for the two systems, micelles and liposomes, by using PEG-modified phospholipids were carefully monitored by optical, morphological and structural investigation. The hydrodynamic diameter and the colloidal stability of both micelles and liposomes loaded with PbS NCs, were evaluated by using Dynamic Light Scattering (DLS) and ζ -Potential experiments, resulting satisfactorily stable in physiological media. The cytotoxicity of the resulting PbS NC loaded nanovectors was assessed by *in vitro* investigation on Saos-2 cells, indicating a toxicity of the PbS NC loaded liposomes lower than that found for the micelles with the same NC cargo, reasonably due to the different overall composition of the two prepared nanocarriers. Finally, the cellular uptake in the Saos-2 cells of both the NC containing systems was evaluated by means of confocal microscopy studies by exploiting a visible fluorescent phospholipid and demonstrating the ability of the both luminescent nanovectors to be internalized. The obtained results envision the great potential of the prepared emitting nanoprobe for imaging applications in the second biological window.

Introduction

Novel biomedical imaging techniques, such as computed tomography (CT), positron emission tomography (PET), magnetic resonance imaging (MRI), ultrasound and optical imaging, represent nowadays important tools for the early detection and diagnosis of diseased tissues. Among these imaging tools, photoluminescence (PL) based biomedical imaging offers clear advantages in terms of prompt feedback, high sensitivity, and high resolution, though low penetration depth of light in biological tissues represents a significant limitation.^{1,2}

Typically, luminescence from probes emitting in the visible range (400–700 nm) can have only a shallow penetration into the tissue (approximately 1mm) due to the high absorption coefficients of blood, skin and fatty tissue and the scattering of the photons. Near infrared (NIR) fluorophores however, may overcome such limitations. NIR light indeed, can penetrate biological tissues more deeply (down to millimetres and even centimetres scale) and more efficiently respect to visible light

due to the lower absorption and scattering. In addition, the biological autofluorescence is minimum at these wavelengths.^{3,4} The biological tissues and water in the NIR region are characterized by two main optical transparency regions, the so-called first (NIR-I, 650-950 nm) and second (NIR-II, 1000-1400 nm) windows defined by a local minimum in their absorption spectra.^{4,5} Simulations and modelling studies of optical imaging in turbid media, such as tissue or blood, suggested that it would be possible to improve signal-to-noise ratios by over 100-fold by using fluorophores that emit light in NIR-II window.^{4,5} In this context, NIR-II emitting nanocrystal (NC)-based imaging probes are expected to provide enhanced medical diagnostic tools based on their superior brightness and photostability compared with conventional molecular probes.³⁻⁶ However, the synthesis of NCs emitting in the NIR-II window still remains restricted to a few materials, such as PbSe, PbS, CdHgTe and Ag₂S, and the design of novel emitters for NIR-II biomedical imaging is an urgent task.⁷⁻¹¹ In this framework, PbS based NCs are promising candidates for imaging in this advantageous region of the electromagnetic spectrum. However, the *as-synthesized* colloidal PbS NCs are generally not water-dispersible and therefore not suitable to be applied in a biological environment. Moreover, the potential toxicity of lead based NCs requires to be suppressed with proper surface modification to make them biocompatible.¹² Lipid micro-heterogeneous systems like micelles and liposomes are widely used for both *in vitro* and *in vivo* delivery of drugs, proteins, genes, nutraceuticals and also for bioconjugation and delivery of nanomaterials.¹³⁻¹⁵ The NC insertion into phospholipid-based micelles and liposome offers several advantages, such as colloidal stability and retention of their peculiar optical properties in aqueous media, as well as

^a Istituto per i Processi Chimico-Fisici-CNR UOS Bari, Via Orabona 4, 70125 - Bari, Italy.

^b Università degli Studi di Bari Aldo Moro, Dipartimento di Chimica, Via Orabona 4, 70125 - Bari, Italy.

^c CNR, Institute of Nanotechnology (NANOTEC), Dipartimento di Chimica, Università degli Studi di Bari Aldo Moro Via Orabona 4, 70125 - Bari, Italy.

^d Università degli Studi di Bari Aldo Moro, Dipartimento di Farmacia – Scienze del Farmaco, Via Orabona 4, 70125 - Bari, Italy.

† These authors contributed equally.

* Corresponding authors n.depalo@ba.ipcf.cnr.it, v.deleo@ba.ipcf.cnr.it

Electronic Supplementary Information (ESI) available: [Vis-NIR absorption and PL spectra of PbS NCs, before and after their incorporation in lipid based nanovectors, and FTIR-ATR spectrum of pure OLEA and pure DDT cast from organic solvent]. See DOI:10.1039/x0xx00000x

ARTICLE

Journal Name

high-efficiency for intracellular delivery, wide availability and cost effectiveness.¹³ Furthermore, micelles and liposomes can be loaded with drugs, proteins and other bioactive molecules for theranostic applications and can be further decorated at the surface with peptides, antibodies and other targeting entities to promote their active delivery in cells.^{16,17}

In this work, hydrophobic PbS NCs emitting in the NIR-II window were functionalized with polyethylene glycol (PEG) grafted phospholipids, by means of their encapsulation in two distinct microheterogeneous systems, and in particular, in the core of micelles and in the bilayer of liposomes. The PEG termination, provides a hydrophilic protective layer at the NC containing micelle or liposome surface, and it is expected to limit the natural opsonisation process of the particle in the blood, thus preventing the further recognition by macrophages, and finally increasing their half-life in blood.¹⁸ Photoluminescence spectroscopy (PL) proved that the emission of NCs was retained after their encapsulation in the two different lipid based nanostructures, while their morphology, size and stability before and after PbS NCs incorporation were comprehensively characterized by Transmission Electron Microscopy (TEM), dynamic light scattering (DLS) and ζ -potential investigation. Cytotoxicity evaluation of PEG-lipid micelles and liposomes loaded with PbS NCs was performed both by means of cell viability assessment and cell morphology investigation on human Saos-2 osteoblast cell line. Finally confocal microscopy study successfully demonstrated their ability of both the PbS NC loaded nanocarriers, though different for the two systems, to be internalized by Saos-2 osteoblast cells, that thus representing potential candidate effective as bio-imaging agents in the NIR-II window.

Experimental Section

Materials

Lead (II) oxide (PbO, powder 99.99%), hexamethyldisilathiane (HMDS, synthesis grade), 1-octadecene (ODE, 90 % technical grade), oleic acid (OLEA, technical grade 90 %), trioctylphosphine (TOP, 90 % technical grade), Sephadex G-50 medium, cholesterol (CH), dodecanethiol (DDT, 97 %), sodium cholate (SC), the reagent grade salts for the 50 mM K-phosphate/100 mM KCl (pH 7.0) buffer solutions, phosphotungstic acid (99.995 %), paraformaldehyde, Triton X100, Fetal Bovine Serum (FBS), 50 IU/mL penicillin, 50 IU/mL streptomycin 200 mM glutamine, trypsin/EDTA solution, MTT powder (3-(4,5-Dimethylthiazol-2-yl)-2,5-diphenyltetrazolium bromide) and MTT solubilisation solution were purchased from Sigma-Aldrich. All solvents, namely ethanol, chloroform also purchased from Sigma-Aldrich, are of the highest purity available. 1,2-Dipalmitoyl-sn-glycero-3-phosphoethanolamine-N-[methoxy(polyethylene glycol)-2000] (16:0 PEG-2-PE), 1,2-Dimyristoyl-sn-Glycero-3-Phosphoethanolamine-N-[Methoxy(Polyethylenglycol)-2000] (14:0 PEG-2-PE), cholesterol (ovine wool, >98 %) and 1,2-distearoyl-sn-glycero-

3-phosphoethanolamine-N-[poly(ethylene glycol)2000-N'-carboxyfluorescein] (18:0 PEG-2-PE-CF) were purchased from Avanti Polar Lipids. Phosphatidylcholine (PC) was from Lipoid. All aqueous solutions were prepared by using water obtained from a Milli-Q Gradient A-10 system (Millipore, 18.2 M Ω cm, at 25 °C, organic carbon content \leq 4mg L⁻¹). Saos-2 osteoblast cell line was from ICLC, Genova, Italy. Dulbecco's modified Eagle's medium (DMEM) was from Sigma Chemical Co. 75 cm² flasks were purchased from Barloworld Scientific, while Coomassie Brilliant Blue R250 (CBB R250) powder from Biorad. For intracellular staining Phalloidin conjugated with TRITC and Fluoroshield with DAPI were purchased from Sigma.

Synthesis of PbS Nanocrystals

Oleic acid capped PbS NCs were synthesized as previously reported in literature.¹⁹ Briefly, 4 mmol of PbO, 9.0 mL of TOP, and 2.7 mL of OLEA were introduced in a three-neck flask containing 36 mL of ODE. The reaction mixture was left stirring under vacuum at 120 °C. Subsequently, a 20 mM solution of HMDS in ODE, with a Pb/S molar ratio of 2:1, was swiftly injected. The temperature was rapidly decreased to 80 °C and the reaction was stopped after 13 minutes. Finally, PbS NCs, collected and purified with ethanol from unreacted precursors, were dispersed in chloroform, achieving a final concentration of 9·10⁻³ M.

PbS Nanocrystal Ligand Exchange

A ligand exchange procedure was carried out in order to replace the pristine OLEA molecules coordinating the PbS NC surface with DDT. 200 μ L of PbS NC chloroform suspension at concentration of 9·10⁻³ M were added into a vial containing 800 μ L of chloroform and 100 μ L of DDT. The resulting mixture was vigorously stirred for 24 h at 40 °C and finally purified by precipitation with the addition of ethanol and centrifugation. The DDT capped PbS NCs, recovered as black precipitate were dispersed in chloroform.

Encapsulation of PbS Nanocrystals in Phospholipid Bilayer of PEG-Modified Liposomes

PbS NC-Liposomes (NC-LIP) were prepared by micelle to vesicle transition (MVT) method as previously described.¹³ Briefly, PC, 14:0 PEG-2-PE and CH (at 1:0.1:0.05 molar ratio respectively) were co-dissolved in chloroform with the defined amounts of DDT PbS NC stock solution (C=8·10⁻³ M) and then dried with a gentle nitrogen flux to form a homogeneous film on the walls of a conical glass tube. Solvent was completely removed under vacuum (24 h). Subsequently, 0.5 mL of 4 % SC in 50 mM K-phosphate/100 mM KCl (pH 7.0) were added to the dry lipid film and then sonicated to form a clear, translucent mixed micelle solution. The latter was loaded into a glass column packed with G-50 Sephadex Medium equilibrated with 50 mM K-phosphate/100 mM KCl for detergent removal by size

exclusion chromatography. Liposomes eluted after void volume of about 1.5 mL.

Encapsulation of PbS Nanocrystals in Hydrophobic Core of PEG-Modified Phospholipid Micelles

PbS NC-Micelles (NM-MIC) were achieved by dissolving defined amounts of DDT PbS NC stock solution ($C=8 \cdot 10^{-3}$ M) with $5.5 \cdot 10^{-6}$ mol of 16:0 PEG-2-PE in chloroform. A dried NC/PEG-lipid layer was attained by solvent evaporation under N_2 flux and then kept under vacuum for 1 hour. Phosphate buffer solution was added to the dried NC/PEG-lipid film and the resulting aqueous solution was repeatedly heated to 80 °C and subsequently cooled to room temperature. Finally, micelles were purified by centrifugation and filtration.¹⁵

Preparation of Visible Fluorescently Labelled Liposomes or Micelles

Fluorescently labelled PbS NC-LIP and PbS NC-MIC were prepared by adding 0.4 % of 18:0 PEG-2-PE-CF, characterized by visible emission ($\lambda_{Ex}/\lambda_{Em}=485\text{nm}/523\text{nm}$), to the lipid blend.

Preparation of Empty Liposomes and Micelles

Empty liposomes (LIP) and micelles (MIC) were achieved by following the same protocols previously described for the preparation of NC containing liposomes and micelles respectively, just without adding the NCs.

Cell Culture

Cell culture experiments were performed by using the human Saos-2 osteoblast cell line. Cells were routinely grown in Dulbecco's modified Eagle's medium (DMEM) supplemented with 10 % heat-inactivated foetal bovine serum (FBS), 50 IU/mL penicillin, 50 IU/mL streptomycin and 200 mM glutamine, and maintained at 37 °C in a saturated humid atmosphere containing 95 % air and 5 % CO_2 in 75 cm^2 flasks. Cells were detached with a trypsin/EDTA solution, re-suspended in the medium and seeded within wells of 24 well plates for incubation experiments at a concentration of 1×10^5 cells/well.

Cytotoxicity Assays

After 24 h of incubation, 3 wells per incubation time per process were used to evaluate cell viability and proliferation with the MTT assay. The complete medium was removed and 1 mL of fresh complete medium with 100 μ L of 5 mg/mL MTT solution was added. The solution was prepared by dissolving 100 mg of MTT in 20 mL of DMEM without serum and phenol red. The resulting medium was incubated (37 °C, 2h) to allow MTT to penetrate the cells, react with the mitochondrial succinate dehydrogenase, and form the dark blue formazan product. Then, 1 mL of the MTT solubilisation solution was added to dissolve formazan and the optical density (O.D.) of

the resulting solution was read at 570 nm after subtracting the background absorbance at 690 nm.²⁰ Since reduction of MTT can only occur in metabolically active cells, the level of activity is a measure of the viability of the cells.

Two wells per time per process were used for staining cells with a CBB solution, which forms protein-dye complex at the cell membrane, and thus investigate cell morphology. The solution was prepared by mixing 2 g of CBB R250 powder, 450 mL of methanol, 450 mL of deionized water, and 10 mL of acetic acid. After removal of the culture medium, cells were fixed with 4 % paraformaldehyde (PFA)/PBS solution for at least 20 min, rinsed twice with PBS and stained with CBB for 3 min. This solution was rinsed with PBS until a clear solution was obtained. An inverted microscope (Leica DM IL) was used to investigate cells at different magnifications.

Cell viability data presented in this study are reported as mean values \pm standard deviation (SD). Each experiment was repeated at least three times. Statistical analysis was performed using two-way ANOVA followed by Bonferroni post hoc test by means of the GraphPad Prism Software (GraphPad Software, Inc.). Differences were considered significant with a p value lower than 0.05.

Photophysical Characterization

Vis-NIR absorption spectra were recorded by using a Cary Varian 5000 UV-visible-NIR spectrophotometer. The measurements were carried out by using optically coupled quartz cuvettes, firstly recording the baseline (solvent vs solvent) and, successively, the sample spectrum (sample vs solvent), in order to minimize the solvent absorption in the zone of interest. PL emission measurements were acquired by using a Horiba Jobin Yvon Fluorolog-3 spectrofluorimeter, supplied of a 450 Xe lamp as an excitation source, coupled to a double grating (blazed at 300 nm) Czerny-Turner monochromator for wavelength selection. The detection system consists of a TBX-PS photon counter detector in the visible range and a Peltier-cooled InGaAs detector in the NIR range.

ATR-FTIR Spectroscopy

Mid-infrared spectra were acquired with a Perkin-Elmer Spectrum One FTIR spectrometer equipped with a deuterated tryglycine sulfate (DTGS) detector. The spectral resolution used for all experiments was 4 cm^{-1} . For ATR measurements, the internal reflection element (IRE) used was a three-bounce 4-mm-diameter diamond microprism. Sample films were cast directly on the internal reflection element by depositing the solution of interest (3-5 μ L) onto the upper face of the diamond crystal and allowing the solvent to evaporate.

Particle size, size distribution and surface charge

Hydrodynamic diameter (size), size distribution and colloidal stability of empty and NC containing micelles or liposomes were detected using a Zetasizer Nano ZS, Malvern Instruments

ARTICLE

Journal Name

Ltd., Worcestershire, UK (DTS 5.00). In particular, size and size distribution were determined by means of dynamic light scattering (DLS) after dilution of micelle or liposome aqueous solutions (phosphate buffer, 10 mM, pH 7.4) in demineralized water. Size distribution is described in terms of polydispersity index (PDI). The ζ -potential measurements, *i.e.* the surface charge, were performed by means of a laser Doppler velocimetry (LDV) after dilution of micelle or liposome aqueous solutions (phosphate buffer, 10 mM, pH 7.4) in KCl aqueous solution (1 mM). All reported data are presented as mean values \pm standard deviation of three replicates.

Transmission Electron Microscopy

The NC morphology was assessed with both Transmission Electron Microscopy (TEM) and High-Resolution TEM (HR-TEM). Particularly, TEM micrographs were recorded by using a Jeol JEM-1011 microscope, working at an accelerating voltage of 100 kV, and acquired by an Olympus Quemesa Camera (11 Mpx). In addition, HRTEM images were acquired using a JEOL 1100 microscope operating at 200 kV. For both analysis, the samples were prepared by dropping on 400 mesh amorphous carbon-coated Cu grid the PbS NC chloroform dispersion or, alternatively, the PbS NC-MIC or PbS NC-LIP aqueous suspension, and letting the solvent to evaporate. The samples demonstrated to be stable under the electron beam, without degrading within the typical observation times. Size statistical analysis of the NC based samples was performed by means of the freeware *ImageJ* analysis program. In particular, the average NC size and the relative standard deviation ($\sigma_{\%}$) were determined to define the NC size distribution. Positive staining TEM experiments were performed by dipping the grid, after the NC based sample deposition in a 2 % (w/v) phosphotungstic acid solution for 30 seconds. Staining agent excess was removed from the grid by rinsing with ultrapure water (dipping the grid in ultrapure water three times for 10 seconds). The sample on the grid was left to dry overnight and finally stored in a vacuum chamber until analysis.

Confocal Microscopy

Human Saos-2 osteoblast cells cultured on glass coverslips were incubated for 1 hours in DMEM containing PbS NC-MIC or PbS NC-LIP, alternatively at the final phospholipid concentration of 0.6 mg/mL. The tested PbS NC concentration was 2 μ M for both samples. After incubation, the culture medium was removed and cells were rinsed three times with PBS-buffer and then fixed with 4 % w/v paraformaldehyde in PBS buffer (30 min). After two washing cycles with PBS buffer, cells were permeabilized with Triton X-100 0.1 % in PBS for 25 min, and washed again with PBS buffer. After incubation with the TRITC-conjugated Phalloidin cells were coated with a drop of DAPI containing Fluoroshield and covered with a glass coverslip. Laser scanning confocal microscopy was performed by using a Leica TCS SP8 X (Leica Microsystems, Germany)

inverted confocal microscope using a $\times 63$, 1.40 numerical aperture oil immersion lens for imaging. Laser beams with 405, 488 and 568 nm excitation wavelengths were used for DAPI, visible fluorescently labelled PbS NC-LIP or PbS NC-MIC and Phalloidin-TRITC imaging, respectively. Differential interference contrast (DIC) microscopy was used to highlight cellular boundary. Confocal images were recorded by using sequential scanning to exclude possible cross-talks in addition six line average was used to increase signal to noise response. All data were processed with Leica LAS AF LITE software (Leica microsystems, Germany).

Results and discussion

Two different lipid based nanosized carriers were designed and prepared to specifically attain dispersibility and stability of hydrophobic NIR emitting PbS NCs in aqueous media. Namely, organic capped PbS NCs were synthesized and successfully encapsulated both in the hydrophobic core of PEG-modified lipid micelles and in the hydrophobic bilayer of liposomes, by take advantage, for both systems, of the interdigitation among lipid hydrophobic tails and the alkyl chains of the NC capping agents. The ligand exchange reaction was found crucial for the successful incorporation of the PbS NCs either in the micelles and in the liposomes. In fact, the native OLEA and TOP capping ligands of the PbS NCs, deriving from the synthetic procedure, were proven ineffective for the encapsulation of PbS NCs into the hydrophobic domain of the investigated phospholipid based nanosystems. Such an issue can be reasonably explained considering the steric hindrance of the three alkyl chains in the TOP molecules and the unsaturated alkyl chain of *cis*-OLEA molecules. Such alkyl chains result loosely packed, thus making ineffective the hydrophobic interdigitation with the lipid tails of micelles and bilayer structures. In fact the precipitation of the OLEA/TOP capped PbS NCs in aqueous solution occurs, both for liposomes and PEG-modified phospholipid micelles, demonstrating as the lipid structures resulted inadequate to provide a shield against the aqueous environment and highlighting the crucial role played by capping ligand at NC surface, as observed elsewhere.^{13,21,22} For example, a very similar behaviour was observed in the incorporation of the trioctylphosphine oxide (TOPO) coated CdSe@ZnS NCs in liposomes by the MVT technique.¹³ A suitable NC surface functionalization is thus necessary to promote the effective incorporation of NCs into the lipid micro-heterogeneous systems. The OLEA/TOP molecules at NC surface were therefore replaced with DDT ones. The linear DDT molecules were selected to replace the pristine NC ligands, thanks to their specific chemical and geometrical characteristics, considering the high affinity of the thiol moiety for the PbS NC surface and the optimal hydrophobic interactions among their linear alkyl chains and the phospholipid tails.¹³

A scheme depicting the steps leading to the encapsulation of DDT capped PbS NCs in the core of micelles or in the bilayer of liposomes is reported in Chart 1.

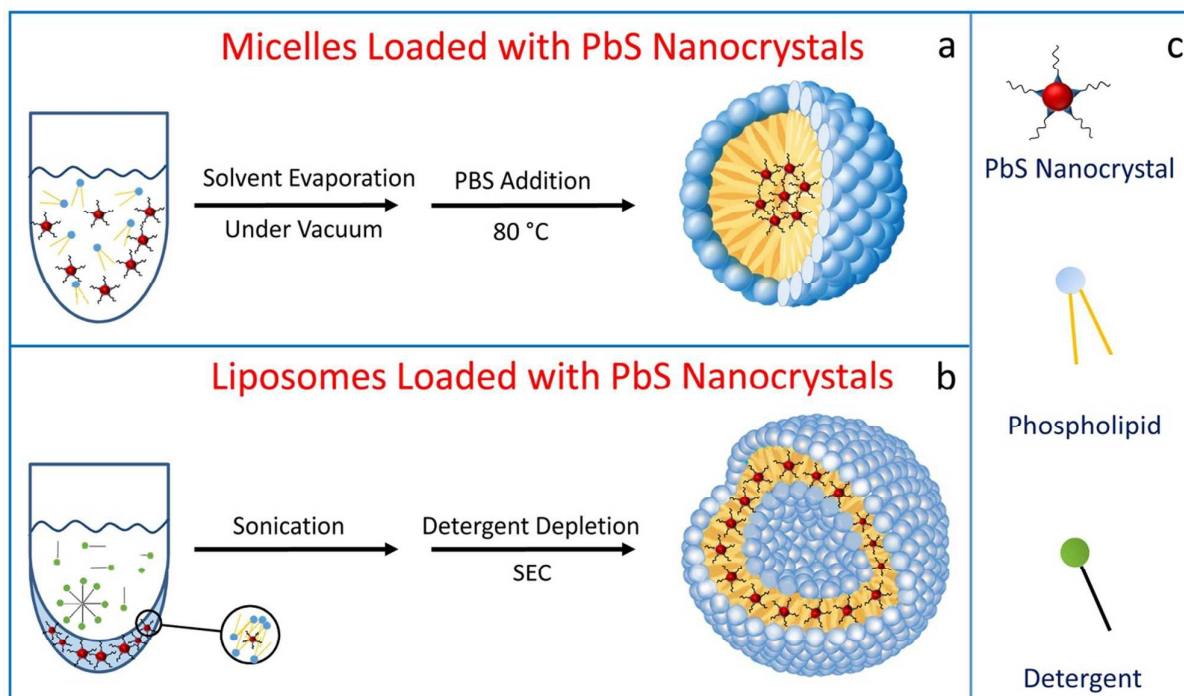


Chart 1. General scheme for the PbS NC functionalization process leading to the formation of PEG-modified phospholipid micelles (a) and liposomes (b). List of the single sketches depicted in the charts a and b. The sketches intend to provide just a pictorial and qualitative description of the proposed procedures, being also the dimensions of the different components not to scale (c).

Structural and Spectroscopic Characterization of Organic Coated PbS Nanocrystals before and after Ligand Exchange Reaction

The organic capped PbS NCs, before and after the ligand exchange reaction, were characterized by optical absorption and emission, as well as FTIR-ATR spectroscopy, TEM and HR-TEM measurements (Figure 1). The absorption spectrum of the OLEA/TOP capped PbS NCs, synthesized as previously reported by Corricelli et al.,¹⁹ clearly shows a well-resolved excitonic transition signal (Figure S1(a)), at 779 nm; the corresponding photoluminescence (PL) emission spectrum is characterized by the presence of a single narrow emission peak, centred at 844 nm, thus in the NIR-I window of the electromagnetic spectrum, which can be ascribed to electron-hole band edge recombination (Figure 1a). The TEM investigation reveals the formation of PbS NCs with a narrow size-distribution, as also confirmed by the corresponding size distribution histogram (Figure 1c and Figure 1g, respectively). The statistical analysis provides an average diameter of 2.3 ± 0.5 nm, corresponding to $\sigma_{\%} = 7\%$ (see the corresponding histogram in Figure 1g). Both TEM and HR-TEM analysis (see the micrographs in Figure 1c and 1e, respectively) confirm the high crystalline quality of the as-prepared PbS NCs. Interestingly, the PL investigation on PbS NCs upon the ligand exchange with DDT molecules shows a significant red shift of the emission signal, from the NIR-I to

the NIR-II window (Figure 1b). In fact the emission peak of DDT capped PbS NCs shifts at 1024 nm and appear broader and more asymmetric compared to the one recorded for the OLEA/TOP capped PbS NCs (Figure 1a), as a further NC growth process occurred during the capping exchange. Also the absorption peak (Figure S1(b)) appears broader than that corresponding to OLEA/TOP capped NCs (Figure S1(a)). This hypothesis is supported by the results of the TEM investigation, which demonstrated as DDT capped PbS NCs have an average diameter of 3.2 ± 0.5 nm, thus larger than that of the average diameter of pristine OLEA/TOP capped PbS NCs. HR-TEM micrograph of Figure 1f shows the high crystalline quality of the PbS NCs after the capping exchange procedure. Such a shift could be ascribed to an oriented attachment (OA) mechanism of NCs taking place during the functionalization with thiol. The OA growth is related to the direct self-organization of two particles into a single crystal by sharing a common crystallographic orientation, induced by the replacement of original OLEA/TOP ligands with DDT at NC surface.²³ However, the thorough elucidation of the exact mechanism of the NC growth would require further a more extensive investigation.

ATR-FTIR investigation was carried out in order to assess the post synthetic PbS NCs surface modification before and after the ligand capping exchange. In Figure 1i the spectrum of the

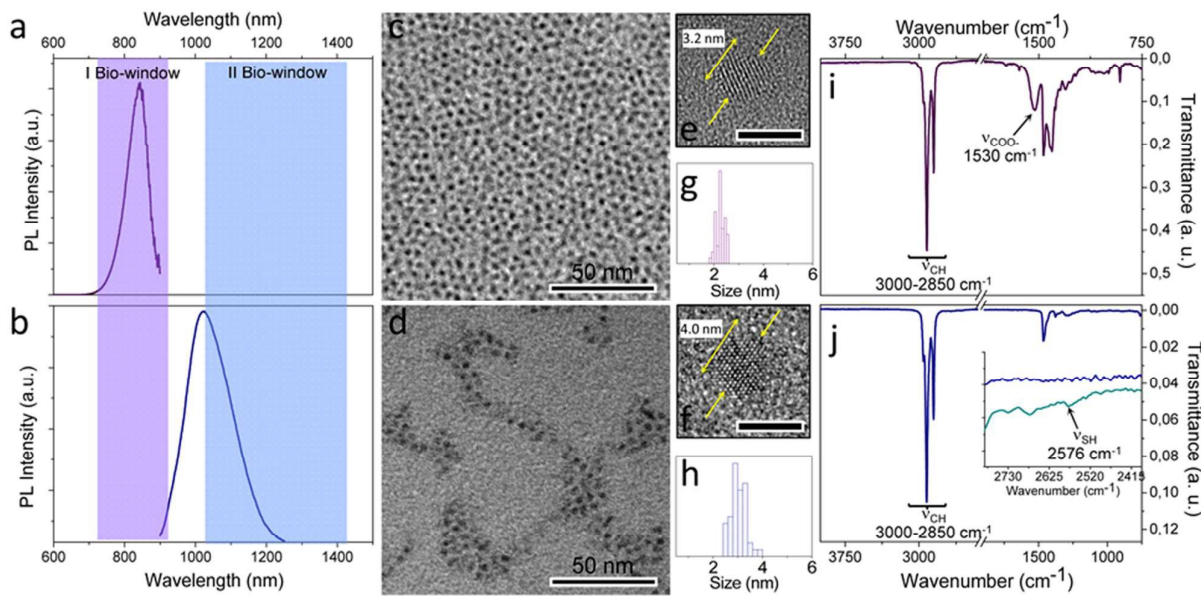


Figure 1. PL emission spectra ($\lambda_{\text{ex}} = 650 \text{ nm}$), TEM and HR-TEM micrographs, histograms of the corresponding size-distribution and FTIR-ATR spectra of OLEA/TOP (a, c, e, g and i, respectively) and DDT (b, d, f, h and j, respectively) capped PbS NCs dispersed in organic solvent. Inset in j: comparison of magnified FTIR-ATR spectra of pure DDT (green) and DDT (blue) capped PbS NCs in the range of $2730\text{--}2415 \text{ cm}^{-1}$.

as-prepared OLEA/TOP capped PbS NCs displays an intense signal at 1530 cm^{-1} , typically ascribed to the stretching of the COO^- group of OLEA molecules, interacting with PbS NC surface through a bidentate bond.^{24,25} The interaction of oleate molecules with PbS NCs is further confirmed by lack of the characteristic vibrations of the C-OH groups at 1710 cm^{-1} , clearly detectable in the pure OLEA spectrum (Figure S2a).

Since the only signal possibly ascribable to TOP molecules is the P- CH_2 vibration which lies above 1400 cm^{-1} , *i.e.* in a very crowded region due to the presence of the aliphatic chain signals, the assignment is very difficult. However, even though no distinctive vibrations can be univocally assigned to TOP molecule coordinating the NC surface, previous works demonstrated the coordination of TOP to the surface of PbS NCs under similar conditions.^{19,26}

The lack of the typical oleate group stretching at 1530 cm^{-1} in the DDT-capped PbS NC spectrum (Figure 1j) allows to infer that, upon the ligand exchange, the OLEA molecules were effectively removed from NC surface. While, the spectrum of the PbS NCs after DDT treatment shows typical distinctive features of the pure DDT (Figure S2b), namely the C-H stretching vibrations of DDT aliphatic chain are present at about 2900 cm^{-1} . In addition, the absence of any weak S-H stretching vibration band at 2576 cm^{-1} in the spectrum of DDT-capped PbS NCs (inset of Figure 1j), with respect to the one recorded on pure DDT, can be reasonably accounted for by the coordination of the S-H to the surface of PbS NCs, as a thiolated form, through a monodentate configuration.^{27,28}

Preparation and Characterization of NC-Micelles and NC-Liposomes loaded with PbS Nanocrystals

PEG-modified lipid micelles and liposomes loaded with DDT-capped PbS NCs were prepared by selecting the suitable lipid composition to achieve two different lipid nanovectors with comparable size and surface charge, which are relevant structural parameters affecting the cellular uptake. Therefore, the total lipid amount was kept constant at value of 0.6 mg/mL for the both investigated types of nanosystems, while different lipid compositions were exploited for the preparation of micelles and liposomes, respectively.

NC-LIP were obtained by using the MVT method and starting from mixed micelles composed of detergent molecules and lipids. Mixed micelles were formed by sonication of a lipid-PbS NC thin film added to a high critical micellar concentration (CMC) detergent solution, thus allowing PbS NCs to remain trapped within the hydrophobic region of the mixed micelles. Finally, the removal of detergent molecules from mixed micelles into the bulk solution by means of the SEC (size-exclusion chromatography) technique promoted the merging of bilayer fragments until closed vesicles are formed.¹³ The lipid molecules employed for the NC-LIP preparation were PC, PEG-2-PE and CH at the molar ratio of 1:0.1:0.05, respectively. PC and CH, two important components of the cellular membranes, are typically used for the conventional preparation of liposomes. The incorporation of CH into the lipid bilayer is expected to improve the physical stability of the liposomes and to reduce the permeability of the lipid bilayer.²⁹ Furthermore, modification of

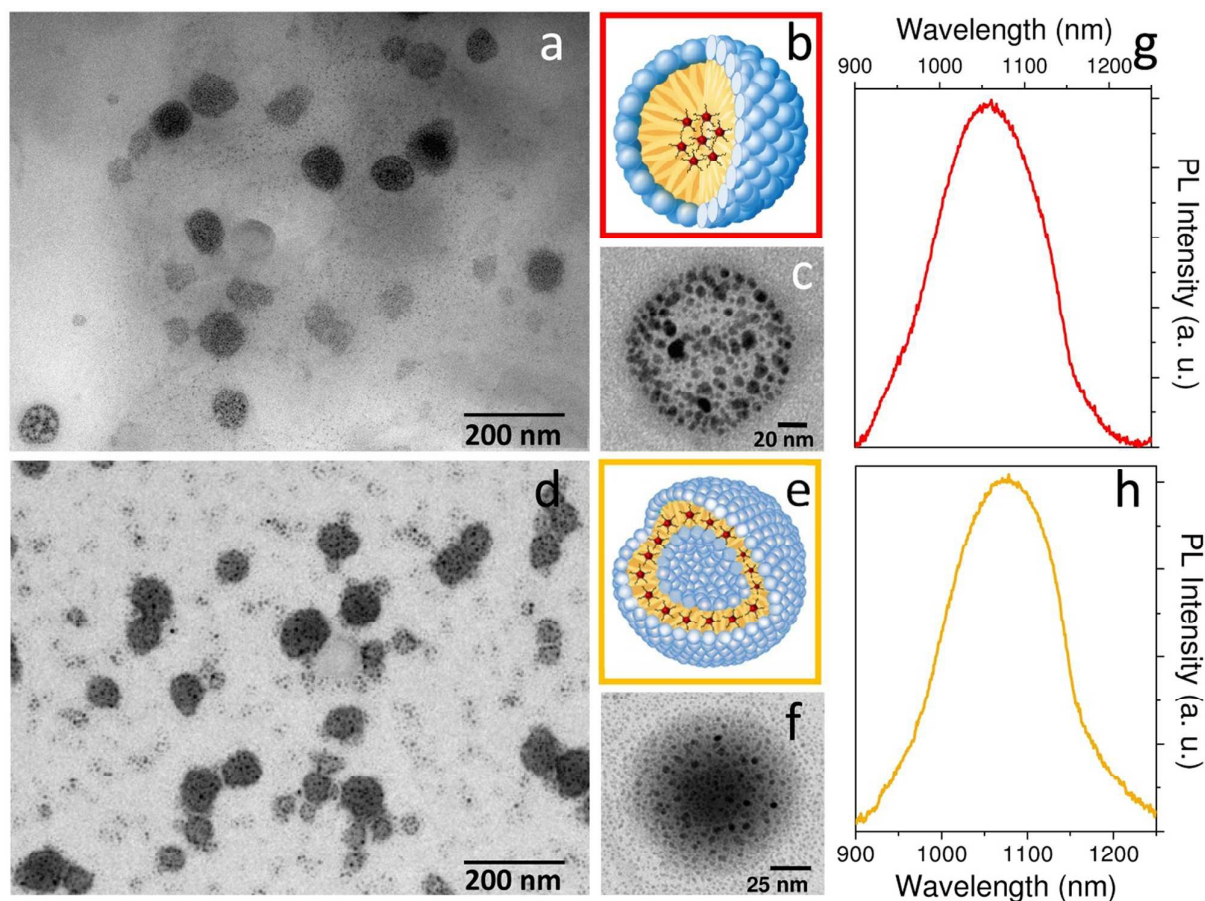


Figure 2. TEM micrographs with positive staining and PL emission spectrum ($\lambda_{ex}=650$ nm) for PbS NC-MIC (a, c and g) and for PbS NC-LIP (d, f and h) dispersed in aqueous PBS buffer. Schematic sketch of DDT capped PbS NCs encapsulated in the hydrophobic core of PEG-modified phospholipid micelles (b) and in the hydrophobic bilayer of liposomes (e).

the liposome surface with PEG-lipids is generally accepted to improve their colloidal stability and their circulation lifetime in the blood. In addition, K. Abe et al. suggested that the enhancement of the PEG-liposome stability by CH integration in their lipid bilayer, is due not only to the increased lipid bilayer fluidity but also to the resulting higher flexibility of the PEG chain, thus ensuring, overall, a longer circulation time in the blood, which is extremely relevant for their *in vivo* applications.²⁹

NC-MIC were attained by using PEG-2-PE. A dried NC/PEG-lipid layer was obtained by chloroform evaporation and hydrated at 80 °C for 20 minutes with intermittent vortex mixing. Subsequently, the solution was allowed to equilibrate at room temperature and purified by centrifugation and filtration.¹⁵ PEG-2-PE represents an optimal candidate for the preparation of micelles useful for *in vivo* applications, thanks to its very low CMC value ($\sim 10^{-6}$ M). Indeed, such a characteristic is relevant for the *in vivo* applications as the residence time of a monomer in a micelle is inversely proportional to the CMC value. Indeed a highly hydrophobic core results in a large activation barrier to the surfactant desorption from the micelle that is often the

rate-limiting step in micelle break-up. Johnsson et al. demonstrated that the formation of spherical micelles can be obtained only starting from neat PEG lipid systems in the dilute region of the phase diagram or realizing a high PEG-lipid concentration in lipid/PEG-lipid systems.^{30,31} PEG-phospholipid, such as PEG-2-PE, induced the formation of mixed micelles, either thread like or discoidal in shape, as well as considerable amount of liposomes, when mixed with different types of lipids, such as PC and CH.^{32,33} Micelles composed of PEG-PE only have a spherical shape and diameter of less than 20 nm. They can efficiently incorporate poorly water soluble drugs into their hydrophobic PE cores, thus protecting them from enzyme degradation and enabling their delivery to tumour sites.^{34,35} In addition, PEG-PE micelles have been also demonstrated able to incorporate hydrophobic NCs with different size, shape and composition in their cores, preserving their size dependent peculiar chemical and physical properties.^{15,36,37}

A structural and morphological investigation of the prepared PbS NCs containing nanovectors, micelles and liposomes, was

ARTICLE

Journal Name

performed by means of TEM and DLS. In addition ζ -potential analysis was carried out in order to get information on their

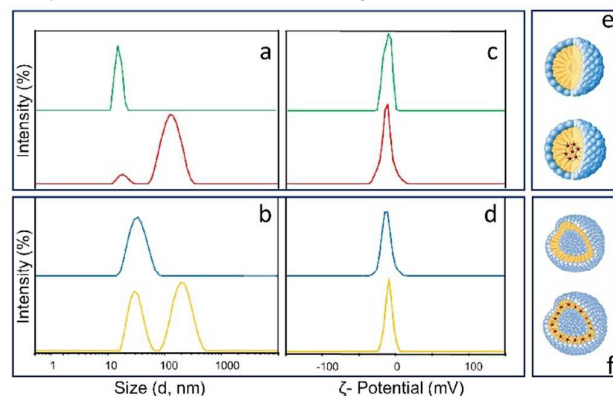


Figure 3. Size distribution by intensity and ζ -potential analysis for empty (a and c, green lines) and PbS NC-MIC (a and c, red lines) and for empty (b and d, blue lines) and PbS NC-LIP (b and d, yellow lines). Schematic sketch of empty and PbS NC-MIC (e) and empty and PbS NC-LIP (f).

surface charge and, hence, on their colloidal stability. TEM micrographs of the positively stained PbS NC containing lipid carriers show structures with diameters ranging from 15 to 120 nm for the PbS NC-MIC (Figure 2a-c) and from 25 to 180 nm for PbS NC-LIP (Figure 2d-f), respectively. These evidences account for the occurrence of lipid based structures in a wide range of sizes, containing a variable number of NCs in each single micelle or liposome. DLS investigation confirmed the findings of the TEM observations, revealing, in addition, a bimodal size distribution for both NC-MIC (Figure 3 a, red line) and NC-LIP (Figure 3b, yellow line). DLS investigation performed on NC-MIC indicates the presence of small structures with an average hydrodynamic diameter of 20 nm, coexisting with larger ones of 130 nm (PDI=0.253±0.007). In the case of NC-LIP sample, the average hydrodynamic diameter was found of 30 and 190 nm (PDI=0.283±0.009) for the smaller and the larger structures, respectively. The size of the small aggregates is compatible with diameters found for the empty micelles and liposomes, respectively (Figure 3a, green line and 3b, blue line), that concomitantly form during the NC encapsulation process in either micelles and liposomes. In addition, the presence of population with a larger average hydrodynamic diameter is consistent with the evidence that a variable number of luminescent PbS NCs can be embedded within one single micelle or liposome, as indicated by the TEM images and as previously reported.^{13,37} The NC multiple occupancy of a micelle or a liposome is, indeed, beneficial for enhancing sensitivity in the imaging of biological systems with respect to a single NC containing micellar or liposomal system,³⁸ as long as the NCs preserve their individuality. The ζ -potential measurements performed on NC-MIC and NC-LIP samples pointed out an overall negative charge at the surface of the both investigated systems, reasonably ascribable to the

phosphate moiety in the structure of phospholipids employed for the preparation of the two different nanosystems.

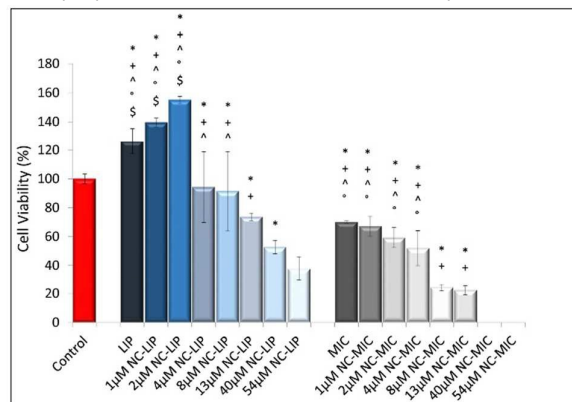


Figure 4. *In vitro* Saos-2 cells viability investigation to assess cytotoxicity of different concentration of DDT PbS NCs after incorporation in PEG-modified lipid micelles and liposomes evaluated by MTT assay at 24 h of growth after 1h incubation Total lipid concentration fixed at 0.6 mg/mL for all tested samples. Two way ANOVA and Bonferroni's post hoc test: *: $p < 0.05$ vs 54 μ M NC; +: $p < 0.05$ vs 40 μ M NC; ^: $p < 0.05$ vs 13 μ M NC; °: $p < 0.05$ vs 8 μ M NC; \$: $p < 0.05$ vs 4 μ M NC

In particular, for NC loaded micelles ζ -potential value of -12.2 ± 0.6 mV was recorded (Figure 3c, red line) and a similar value was also found for empty micelles (Figure 3 c, green line). In the case of NC-LIP (Figure 3 d yellow line) a value of -13.9 ± 0.9 mV was measured, and, similarly, a comparable value was found for empty liposomes. These results indicate a good colloidal stability of both the investigated systems. In addition, the PEG hydrophilic chains exposed at the surface of the lipid-based nanovectors are expected to further enhance their stabilization due to the occurrence of steric effects along with the electrostatic ones.

Interestingly, PL measurements carried out on NC containing lipid systems show that the emitting properties in the II biological window are still retained after their incorporation in the lipid based systems (Figure 1b and d). However a significant red shift of 37 and 50 nm is observed in the PL spectrum of PbS NCs encapsulated in the hydrophobic micelle core or liposome bilayer respectively, when compared to the PL emission band of organic soluble DDT capped PbS NCs. In particular, the PL emission band is found centred at 1061 and 1074 nm for NC-MIC and NC-LIP, respectively (Figure 2 g and h). This behaviour can be explained taking into account that the incorporation process of the emitting NCs in the micelles or in the liposomes confine several NCs into a restricted space, as indicated by TEM investigation, thus reducing their mutual distance. Thus, in this condition, under light excitation energy transfer processes from the smaller NCs to larger NCs become more likely. Such a phenomenon ultimately results in a red shift of maximum emission and in a concomitant inhomogeneous broadening in the low energy side of the signal in the emission spectrum, as can be observed in Fig. 2 g and h.¹³ Also the absorption spectrum appears different from the one of DDT-capped PbS NCs, resulting even broader for

both PbS NCs encapsulated in the hydrophobic micelle core or liposome bilayer (Figure S1(c) and (d)).

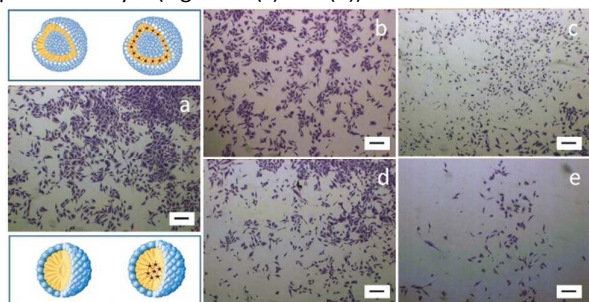


Figure 5. Light microscopy micrographs of Saos-2 cell stained by Coomassie Blue and observed at 24 h after 1 hour incubation with empty liposomes (b) or micelles (d), PbS NC-LIP at PbS NC concentration of 13 μM and (c) PbS NC-MIC at PbS NC concentration of 13 μM (e). Total lipid concentration fixed at 0.6 mg/mL for all tested samples. Control Saos-2 cell in complete DMEM (a). Scale bar 200 μm .

Citotoxicity and uptake studies of PEG-lipid based nanovectors loaded with PbS Nanocrystals

The ability of NC-MIC and NC-LIP to deliver NCs within cells without interfering with cell viability was assessed by means of cyto-compatibility and uptake studies on human Saos-2 osteoblast cell line, which represents a relevant osteoblast model for *in vitro* cell-material based studies.³⁹ Cell viability assays were carried out by treating Saos-2 cells with micelles and liposomes, respectively, at increasing NC cargo, in order to explore an actual PbS NC concentration ranging from 1 to 54 μM .

NC-MIC and NC-LIP at different loading of NCs were obtained starting from an increased amount of stock solution of DDT capped NCs, keeping constant the total lipid amount.¹⁵ In particular, the final lipid concentration was fixed at value of 0.6 mg/mL for all the investigated samples, both micelle and liposome based ones. Then, the Saos2 cells were incubated with the prepared NC loaded nanovectors for 1 hour and the cell viability was estimated by MTT assay at 24 h of growth after the incubation. Empty lipid micelles and liposomes were also tested, in order to evaluate the potential toxicity of the lipid carriers.

The MTT test in Figure 4 clearly shows a different behaviour between cells incubated with the two prepared systems. Saos-2 cultured with empty liposomes (LIP) showed superimposable cell viability of control at 24 h.

On the contrary, cell viability of Saos2 incubated with empty micelles dropped of about 49 % with respect to the control systems ($p < 0.05$). In the case of NC-LIP, the vitality was comparable to that of the control and LIP up to 2 μM concentration of PbS NCs ($p > 0.05$) while a vitality reduction was detected for concentrations higher than 4 μM of PbS NCs, though viability values higher than 60 % were still observed. Finally, with NC-LIP systems at higher NC concentrations (54 μM) a decrease in viability of more than 50 % was recorded.

The NC-MIC affected the cell viability in a concentration-dependent way too. In particular, for the lowest tested concentration values (0-4 μM) the cell viability resulted comparable to that of empty micelles (MIC), being, also in this case, reduced of about 40-50 % respect to the control. A 80 % decrease of cell viability by NC-MIC was found for the NC concentration ranging from 8 to 13 μM . Moving to higher PbS NCs concentration (40-54 μM) no viability was detected attesting for a thorough cytotoxicity of the system at such NC concentrations.

Coomassie blue staining experiment on the Saos2 cells was also performed to assess whether the detected decrease in cell viability was somehow reflected in a different cell morphology. In Figure 5a, Saos2 cells appear typically clustered and very few single cells are visible also after 24 h of cell growth. When cells were exposed to LIP and MIC, after 6 hours only a difference in cell number was noticed, while no change in cell behaviour was detected, since most of the cells appeared clustered together (Figure 5b and 5d). A similar outcome was found for cells incubated with NC-LIP and NC-MIC at PbS concentration ranging from 1 to 8 μM (data not shown). Conversely, a significant change in cell behaviour was detected after cell incubation with NC-LIP or NC-MIC at PbS NC concentration of 13 μM , since Saos2 cells were observed not clustering anymore, but only few spread cells can be finally detected (Figure 5c and 5e). The overall data obtained by cell viability assay and Coomassie blue staining experiment clearly indicate that the response in terms of cytotoxicity of the two NC loaded nanovectors is different. Interestingly, the analysis of cell viability data relating to LIP and MIC, as well as to low tested concentrations of PbS NCs (0-2 μM), seem to suggest that the composition of the phospholipids used for preparation of the two nanosystems can significantly affect the cellular response.

In particular, the different effects on the cells observed for the MIC and LIP, respectively, can be reasonably ascribed only to the different lipid composition of the two nanocarriers. In fact, the overall explored lipid concentration stayed the same (0.6 mg/mL) in the both investigated systems. Furthermore, both lipid based carriers are characterized by very similar negative charge, (-10.04 ± 0.95) and (-10.8 ± 0.73) mV for micelles and liposomes respectively, and comparable average hydrodynamic diameters (namely 20 nm for micelles and 30 nm for liposomes). However, while the micelles were formed exclusively of the synthetic PEG-2-PE molecules, liposome were based on a lipid blend containing also CH and PC which are two important components of the cellular membranes.

A comprehensive study on PEG-PE based micelles interaction with cells, by J. Wang et al., demonstrated the safety of PEG-2-PE in normal cells and highlighted the molecular mechanism underlying their toxicity in cancer cells.³⁴ In particular, PEG-2-PE micelles were found to insert into cell membranes without disrupting membrane integrity and to disassembly at membrane level.

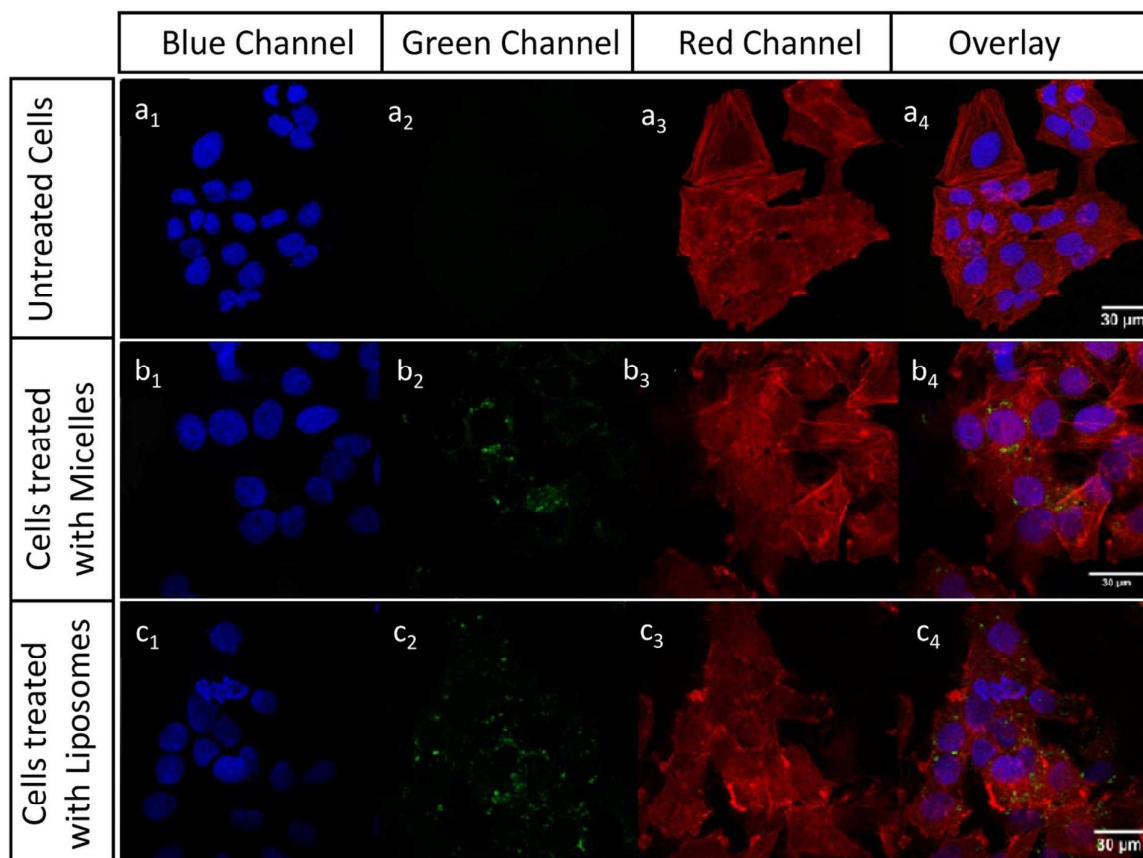


Figure 6. Confocal fluorescence micrographs of fixed Saos-2 cells. Control: untreated cells (Panel a1-a4). Cells images after incubation of Saos-2 cells with fluorescently labelled NC containing liposomes (Panel b1-b4) or micelles (Panel c1-c5). Cells images in the blue (Panel a1, b1, c1), green (Panel a2, b2, c2) and red (Panel a3, b3, c3) detection channel. Overlay of blue, green and red fluorescence (Panel a4, b4, c4). Scale bar 30 μm

The disassembled PEG-PE molecules can be carried into cells through nonspecific endocytosis and finally accumulate in the endoplasmic reticulum (ER), inducing ER stress. Interestingly, under PEG-2-PE induced ER stress, cancer cells initiate proapoptotic signalling while normal cells initiate prosurvival signalling, thus suggesting that PEG-2-PE micelles are suitable carriers for delivery of anticancer drugs. According to these findings, here the observed toxicity of the empty micelles, only formed of PEG-PE, can be reasonably assumed to derive from the disturbance of ER membrane lipid homeostasis due to an accumulation of PEG-PE in the ER, upon their cellular internalization. On the other hand, the higher cell viability observed for the exposure to empty liposomes compared to that of empty micelles may be explained on the basis of a major similarity between the prepared liposomes and natural cell membranes, having the composition of liposomes a PEG-PE content of just 8.7 % weight of the total lipid content. Therefore, the toxicity observed for PbS NC-LIP on Saos 2 cells can be mainly ascribed to the NCs, while the more negative response of the cells treated with PbS NC-MIC can be thought as a result of the combined cytotoxic effect of the PEG-PE molecules and NCs. In fact, for both the lipid based

nanovectors, cell viability was found to decrease at increasing NC content.

These evidences can be explained assuming that cellular internalization by non-specific endocytosis^{35,40} results, both for the micelles and the liposomes, in a release of the NC cargo in the intracellular environment, that turns, at high NC concentration values, in a toxicity level leading to cell damage and death. Different mechanisms were proposed in literature to explain the cell damage due to exposure to inorganic NCs. Among the others, metal ions, released by NCs, were reported to generate free radicals or, alternatively, NC as a whole can induce ROS generation through energy or electron transfer to molecular oxygen.⁴¹ ROS can cause damage to DNA, lipids and other cellular components such as membrane of mitochondria as a consequence induction of apoptosis and necrosis. On the other hands, our recent study on the toxicity effect of CdSe@ZnS NC loaded PEG-PE micelles on primary culture of astrocytes proved that the production of ROS in cells exposed to NC containing micelles is not dependent on the phospholipid concentration, but only on NC concentration.³⁶ While, PEG-PE molecules were demonstrated not responsible of ROS production induced cytotoxicity, in agreement also with Jiang Wang et al. that ascribed the toxicity to endoplasmic

reticulum (ER) stress.³⁵ The effective uptake of NC-MIC and NC-LIP in Saos 2 cells was demonstrated by the confocal microscopy investigation, operating in the visible range. Therefore, a fluorescent probe emitting in the visible region was used to prove the ability of two lipid based nanovectors to be internalized by the cells. Namely, a defined amount of a fluorescent phospholipid bearing a CF ($\lambda_{\text{ex}} = 488 \text{ nm}$) in the structure, and emitting in the visible region was used in the preparation of the NIR emitting NC-MIC and NC-LIP. The cells were incubated for 2 hour with the fluorescently labeled NC-MIC and NC-LIP, prepared at the not toxic NC concentration of 2 μM and at the final phospholipid concentration of 0.6 mg/mL. After the incubation, the cells were fixed and treated with TRITC-Phalloidin or DAPI to stain F-actin and cell nuclei, respectively. Images in blue (Figure 6 Panel a1, b1, c1), green (Figure 6 Panel a2, b2, c2) and red (Figure 6 Panel a3, b3, c3) detection channels are reported in Figure 6 along with the overlay images (Figure 6 Panel a4, b4, c4). The green emission demonstrated the localization in the cells of the CF labelled phospholipid molecules forming the NC loaded micelles and liposomes (Figure 6 Panel b2 and c2), while red (Figure 6 Panel a3, b3, c3) and blue (Figure 6 Panel a1, b1, c1) emission indicated the localization of the actin cytoskeleton and the cell nuclei, respectively. The presence of evident actin stress fibers further highlighted that the uptake of NC by Saos2 cells did not influence cell morphology. The observations made in cellular imaging experiments clearly proved that both the lipid based nanovectors are able to enter the cells.

Conclusions

Hydrophobic PbS NCs, emitting in the NIR-II window, were successfully embedded both in PEG-modified phospholipid micelles and in liposomes, obtaining lipid based nanocarriers with good colloidal stability in aqueous medium. The spectroscopic characterization of thiol capped PbS NCs by means of PL, before and after their encapsulation in micelles or liposomes, proved that their emission properties in the second optical window of the NIR region of the electromagnetic spectrum are retained. The *in vitro* investigation on Saos-2 cells, revealed that the cell viability was affected in a PbS NC concentration-dependent way and that also the phospholipid components significantly influence the cytotoxicity of the two prepared carriers. In particular, cytotoxic activity was shown only for MIC composed of PEG-2-PE, while LIP with a PEG-PE percentage of 8.7 % weight respect to the total lipid content did not affected the cell viability. Finally, confocal microscopy investigation demonstrated the internalization by Saos-2 cells of the NC-MIC and NC-LIP by exploiting a visible fluorescent phospholipid in the NC-MIC and NC-LIP preparation. Therefore, while still more experiments need to be performed to fully assess the viability of such novel bioprobes, this study definitely highlights the potential of the proposed PbS NCs loaded nanovectors as NIR fluorescent probes in the NIR-II window for imaging applications.

Acknowledgements

The work has been partially supported by Nanomax- Integrable sensors for pathological biomarkers diagnosis (N-CHEM), National Sens&Micro LAB (POFESR 2007–2013), NANOfotocatalizzatori per un'Atmosfera più PULita (NANOAPULIA) and by the National PRIN 2012 Prot. 20128ZS2H and Prot. 2012T9XHH7 projects.

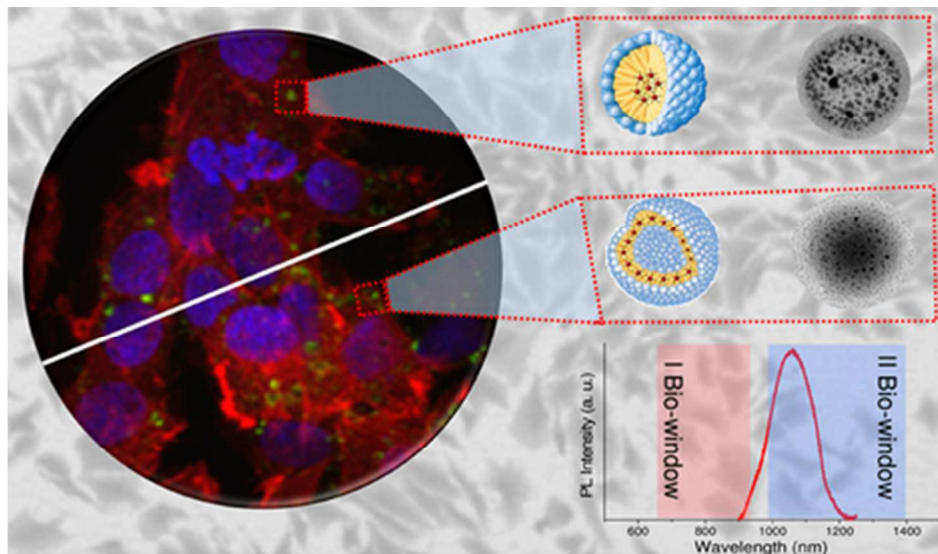
References

- G. Hong, J. T. Robinson, Y. Zhang, S. Diao, A. L. Antaris, Q. Wang and H. Dai, *Angewandte Chemie International Edition*, 2012, **51**, 9818-9821.
- E. Hemmer, A. Benayas, F. Legare and F. Vetrone, *Nanoscale Horizons*, 2016, **1**, 168-184.
- J. Zhou, Y. Yang and C.-y. Zhang, *Chemical Reviews*, 2015, **115**, 11669-11717.
- A. M. Smith, M. C. Mancini and S. Nie, *Nat Nano*, 2009, **4**, 710-711.
- K. Welscher, S. P. Sherlock and H. Dai, *Proceedings of the National Academy of Sciences*, 2011, **108**, 8943-8948.
- R. Wang, X. Li, L. Zhou and F. Zhang, *Angewandte Chemie International Edition*, 2014, **53**, 12086-12090.
- B. L. Wehrenberg, C. Wang and P. Guyot-Sionnest, *The Journal of Physical Chemistry B*, 2002, **106**, 10634-10640.
- L. Bakueva, I. Gorelikov, S. Musikhin, X. S. Zhao, E. H. Sargent and E. Kumacheva, *Advanced Materials*, 2004, **16**, 926-929.
- M. T. Harrison, S. V. Kershaw, M. G. Burt, A. Eychmüller, H. Weller and A. L. Rogach, *Materials Science and Engineering: B*, 2000, **69–70**, 355-360.
- Y. Zhang, G. Hong, Y. Zhang, G. Chen, F. Li, H. Dai and Q. Wang, *ACS Nano*, 2012, **6**, 3695-3702.
- M. Corricelli, N. Depalo, E. Di Carlo, E. Fanizza, V. Laquintana, N. Denora, A. Agostiano, M. Striccoli and M. L. Curri, *Nanoscale*, 2014, **6**, 7924-7933.
- R. Hu, W.-C. Law, G. Lin, L. Ye, J. Liu, J. Liu, J. L. Reynolds and K.-T. Yong, *Theranostics*, 2012, **2**, 723-733.
- V. De Leo, L. Catucci, A. Falqui, R. Marotta, M. Striccoli, A. Agostiano, R. Comparelli and F. Milano, *Langmuir*, 2014, **30**, 1599-1608.
- D. Mastrogiacomo, M. S. Lenucci, V. Bonfrate, M. Di Carolo, G. Piro, L. Valli, L. Rescio, F. Milano, R. Comparelli, V. De Leo and L. Giotta, *RSC Advances*, 2015, **5**, 3081-3093.
- N. Depalo, P. Carrieri, R. Comparelli, M. Striccoli, A. Agostiano, L. Bertinetti, C. Innocenti, C. Sangregorio and M. L. Curri, *Langmuir*, 2011, **27**, 6962-6970.
- B. S. Pattni, V. V. Chupin and V. P. Torchilin, *Chemical Reviews*, 2015, **115**, 10938-10966.
- V. P. Torchilin, *Pharmaceutical Research*, 2006, **24**, 1-16.
- J. V. Jokerst, T. Lobovkina, R. N. Zare and S. S. Gambhir, *Nanomedicine* (London, England), 2011, **6**, 715-728.
- M. Corricelli, D. Altamura, L. De Caro, A. Guagliardi, A. Falqui, A. Genovese, A. Agostiano, C. Giannini, M. Striccoli and M. L. Curri, *CrystEngComm*, 2011, **13**, 3988-3997.
- T. Mosmann, *Journal of Immunological Methods*, 1983, **65**, 55-63.
- P. Fini, N. Depalo, R. Comparelli, M. L. Curri, M. Striccoli, M. Castagnolo and A. Agostiano, *Journal of Thermal Analysis and Calorimetry*, 2008, **92**, 271-277.
- N. Depalo, R. Comparelli, J. Huskens, M. J. W. Ludden, A. Perl, A. Agostiano, M. Striccoli and M. L. Curri, *Langmuir*, 2012, **28**, 8711-8720.
- J. Zhang, Y. Wang, J. Zheng, F. Huang, D. Chen, Y. Lan, G. Ren, Z. Lin and C. Wang, *The Journal of Physical Chemistry B*, 2007, **111**, 1449-1454.
- P. J. Thistlethwaite and M. S. Hook, *Langmuir*, 2000, **16**, 4993-4998.

ARTICLE

Journal Name

- 25 M. Nara, H. Torii and M. Tasumi, *The Journal of Physical Chemistry*, 1996, **100**, 19812-19817.
- 26 K. A. Abel, J. Shan, J.-C. Boyer, F. Harris and F. C. J. M. van Veggel, *Chemistry of Materials*, 2008, **20**, 3794-3796.
- 27 M. Aslam, I. S. Mulla and K. Vijayamohan, *Langmuir*, 2001, **17**, 7487-7493.
- 28 N. K. Chaki and K. P. Vijayamohan, *The Journal of Physical Chemistry B*, 2005, **109**, 2552-2558.
- 29 K. Abe, K. Higashi, K. Watabe, A. Kobayashi, W. Limwikrant, K. Yamamoto and K. Moribe, *Colloids and Surfaces A: Physicochemical and Engineering Aspects*, 2015, **474**, 63-70.
- 30 M. Johnsson and K. Edwards, *Biophysical Journal*, 2003, **85**, 3839-3847.
- 31 M. Johnsson, P. Hansson and K. Edwards, *The Journal of Physical Chemistry B*, 2001, **105**, 8420-8430.
- 32 E. Johansson, M. C. Sandström, M. Bergström and K. Edwards, *Langmuir*, 2008, **24**, 1731-1739.
- 33 M. C. Sandström, E. Johansson and K. Edwards, *Biophysical Chemistry*, 2008, **132**, 97-103.
- 34 J. Wang, X. Fang and W. Liang, *ACS Nano*, 2012, **6**, 5018-5030.
- 35 J. Wang, Y. Wang and W. Liang, *Journal of Controlled Release*, 2012, **160**, 637-651.
- 36 T. Latronico, N. Depalo, G. Valente, E. Fanizza, V. Laquintana, N. Denora, A. Fasano, M. Striccoli, M. Colella, A. Agostiano, M. L. Curri and G. M. Liuzzi, *PLoS ONE*, 2016, **11**, e0153451.
- 37 G. Valente, N. Depalo, I. de Paola, R. M. Iacobazzi, N. Denora, V. Laquintana, R. Comparelli, E. Altamura, T. Latronico, M. Altomare, E. Fanizza, M. Striccoli, A. Agostiano, M. Saviano, A. Del Gatto, L. Zaccaro and M. L. Curri, *Nano Research*, 2016, **9**, 644-662.
- 38 K.-T. Yong, I. Roy, R. Hu, H. Ding, H. Cai, J. Zhu, X. Zhang, E. J. Bergey and P. N. Prasad, *Integrative Biology*, 2010, **2**, 121-129.
- 39 E. M. Czekanska, M. J. Stoddart, R. G. Richards and J. S. Hayes, *European Cells and Materials*, 2012, **24**, 1-17.
- 40 C.-J. Wen, L.-W. Zhang, S. A. Al-Suwayeh, T.-C. Yen and J.-Y. Fang, *International Journal of Nanomedicine*, 2012, **7**, 1599-1611.
- 41 L. Yan, Z. Gu and Y. Zhao, *Chemistry – An Asian Journal*, 2013, **8**, 2342-2353.



39x23mm (300 x 300 DPI)